Supplementary Information

A Relationship between Three-dimensional Surface Hydration Structure and Force Distribution Measured by Atomic Force Microscopy

K. Miyazawa[1], N. Kobayashi[1], M. Watkins[2], A. L. Shluger[3], K. Amano[4] and T. Fukuma[1,5]

[1]Division of Electrical Engineering and Computer Science, Kanazawa University, Kakuma-machi, Kanazawa 920-1192, Japan

[2]School of Mathematics and Physics, University of Lincoln, Brayford Pool, Lincoln LN6 7TS, United Kingdom

[3]Department of Physics and Astronomy and London Centre for Nanotechnology, University College London, Gower Street, London, WC1E 6BT, United Kingdom

[4]Department of Energy and Hydrocarbon Chemistry, Graduate School of Engineering, Kyoto University, Kyoto 615-8510, Japan

[5]ACT-C, Japan Science and Technology Agency, Honcho 4-1-9, Kawaguchi 332-0012, Japan

*Corresponding author e-mail: fukuma@staff.kanazawa-u.ac.jp
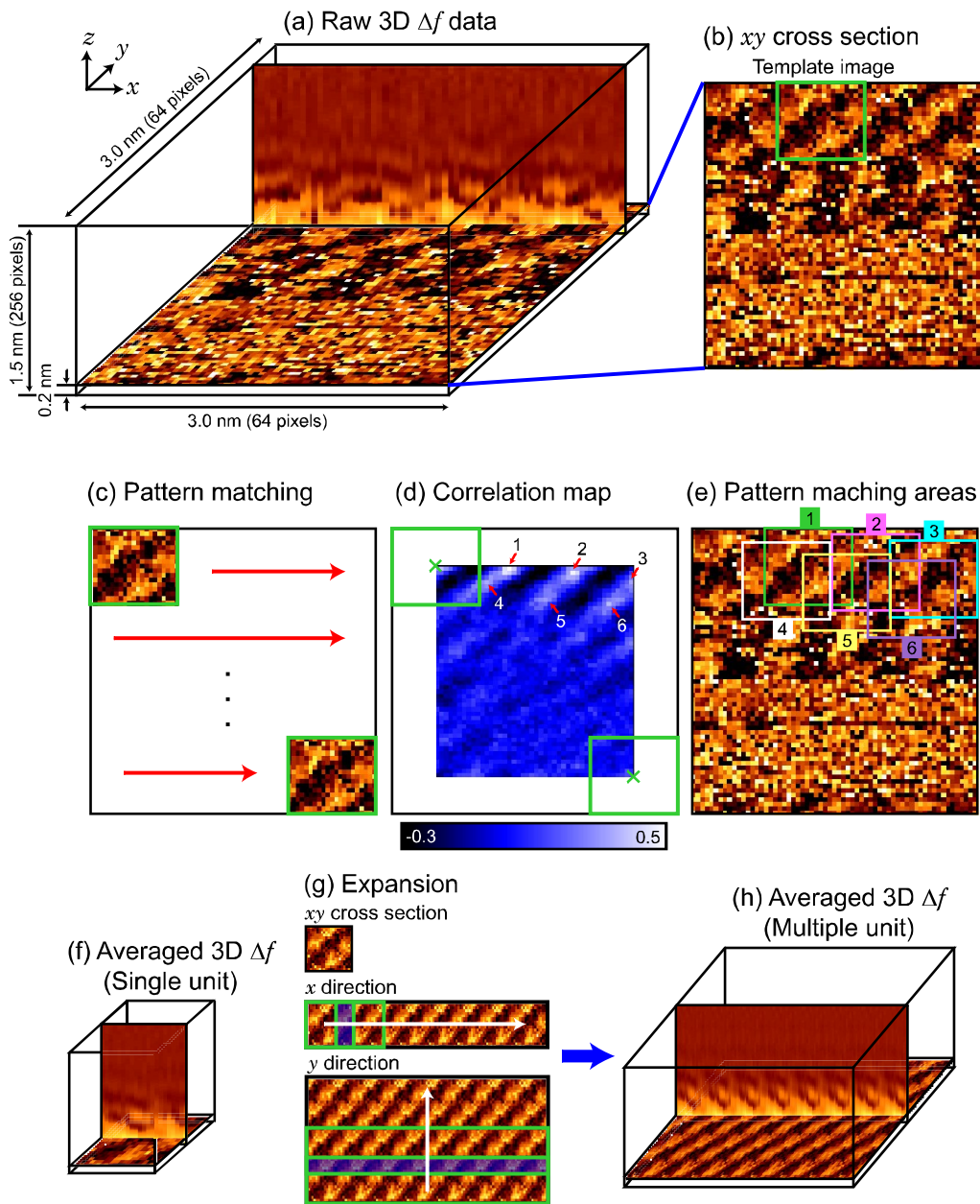
Supplementary Figures

Figure S1: Schematic illustrations showing the average filtering process with the pattern matching algorithm. (a) Raw 3D $\Delta f(r)$ image obtained at a fluorite(111)-water interface by 3D-SFM. (b) xy cross section of the 3D image shown in (a) at $z = 0.2$ nm. The green square shows the location of the template image used for the pattern matching. (c) Scan trajectory of the template image during the pattern matching. (d) Distribution of correlation coefficient between the template image and the original image at each xy position. (e) Selected areas showing good pattern matching ($c > 0.3$). (f) Averaged 3D $\Delta f(r)$ image with a size of the template image. (g) 3D data expansion in xy directions. (h) Expanded averaged 3D $\Delta f(r)$ image.

Figure S1a shows a 3D $\Delta f(r)$ image measured by 3D-SFM. Figure S1b shows an *xy* cross section obtained at *z* position (*z* = 0.2 nm) close to the sample surface. In the upper half of the *xy* cross section, we can see periodic contrasts similar to the structure of fluorite(111) surface. However, contrasts in the middle of the *xy* cross section are not clear. In addition, there is almost no contrast in the lower half of the *xy* cross section.

First, we select a template image with a size slightly larger than the unit cell of a fluorite(111) surface. The template image is scanned in the *xy* cross section as shown in Figure S1c. During the scan, we calculate correlation coefficient (c, Equation (1)) between the template and original images at each *xy* position to obtain a correlation map as shown in Figure S1d.

$$c = \frac{\displaystyle\sum_{j=1}^{M}\sum_{i=1}^{N}\{I(i,j) - \mu_I\}\{T(i,j) - \mu_T\}}{\sqrt{\displaystyle\sum_{j=1}^{M}\sum_{i=1}^{N}\{I(i,j) - \mu_I\}^2 \sum_{j=1}^{M}\sum_{t=1}^{N}\{T(i,j) - \mu_T\}^2}} \tag{1}$$

$$\mu_I = \frac{1}{NM}\sum_{j=1}^{M}\sum_{i=1}^{N}I(i,j), \mu_T = \frac{1}{NM}\sum_{j=1}^{M}\sum_{i=1}^{N}T(i,j)$$

Here, N and M denote pixel sizes of the cross section in *x* and *y* directions, respectively. I and T denote $\Delta f(r)$ value in the template and original images, respectively. From the results of S1d, we found six locations showing a high c value (> 0.3) in the upper half of the *xy* cross section. We obtained an averaged 3D $\Delta f(r)$ image from the six images at the selected areas.

Secondly, we expanded the averaged 3D $\Delta f(r)$ image by repeating it in *xy* directions as shown in Figure S1g. For smoothing out possible discontinuity at the boundaries between two adjacent images, we used averaged values at the overlapped regions indicated by the blue background color in Figure S1g. In this way, we obtained an averaged 3D $\Delta f(r)$ image with a sufficient size for the comparison with theoretically obtained ones.
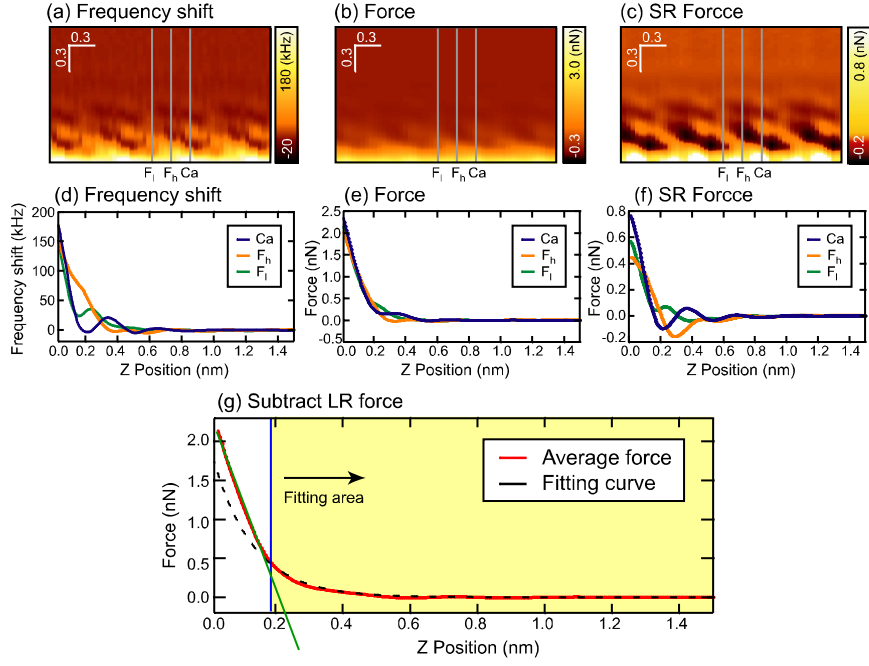
Figure S2: *z* cross sections obtained from the (a) $\Delta f(r)$, (b) $F_{exp}(r)$ and (c) SR $F_{exp}(r)$ images. *z* profiles over Ca, F_h and F_l sites obtained from the (d) $\Delta f(r)$, (e) $F_{exp}(r)$ and (f) SR $F_{exp}(r)$ images. (g) $F_{exp}(r)$ curve averaged over the *xy* area corresponding to the 3D image and the fitted exponential curve.

Figures S2a and S2d show *z* cross section and *z* profiles obtained from the averaged 3D $\Delta f(r)$ image. Figures S2b and S2e show the *z* cross section and *z* profiles obtained from the 3D $F_{exp}(r)$ image. These results show that, local contrasts in the $F_{exp}(r)$ image are relatively weak compared with those in the $\Delta f(r)$ image. Thus, we subtracted the LR force component from the $F_{exp}(r)$ image. We assumed that the LR force is expressed by an exponential function and it does not depend on the local *xy* position. We fitted an exponential curve to the averaged $F_{exp}(r)$ profile to obtain the LR force profile (black dotted line in Figure S2g). The averaged $F_{exp}(r)$ profile shows almost linear distance dependence in the *z* range below 0.2 nm. Thus, we performed the fitting in the *z* range above 0.2 nm as indicated by the yellow background in Figure S2g. We obtained the SR F_{exp} image by subtracting the fitted curve from the $F_{exp}(r)$ profiles at each *xy* position. Figures S2c and S2f show the *z* cross section and *z* profiles obtained from the 3D SR $F_{exp}(r)$ image. These images and profiles show local $F_{exp}(r)$ variations reflecting the sample hydration structure.
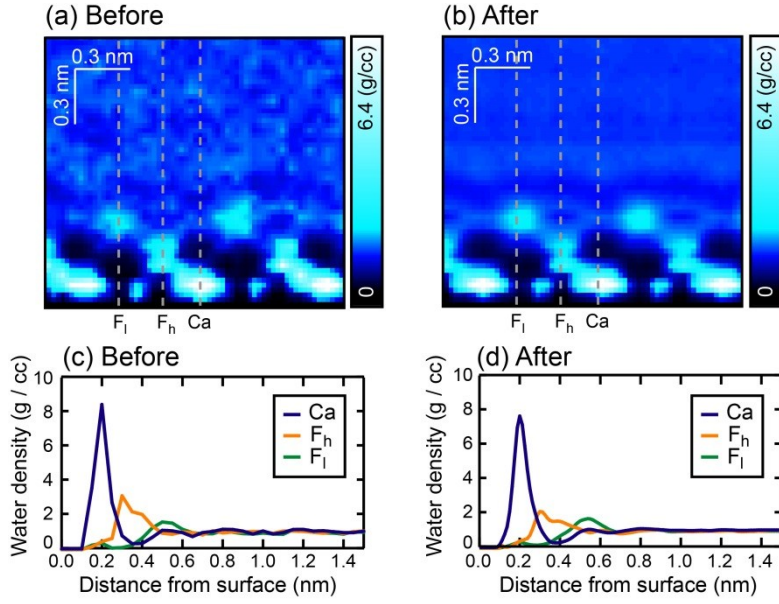
Figure S3: z cross sections and z profiles of $\rho(r)$ distribution calculated by MD simulation (a)(c) before and (b)(d) after the averaging, respectively.

The 3D water density ($\rho(r)$) image was calculated by MD simulation using a simulation box larger than the unit cell of fluorite(111) surface. In the simulated image, even at equivalent positions in the unit cell, the $\rho(r)$ values show variations as shown in Figure S3a. This is due to the finite MD simulation time for averaging the water distribution. To reduce such variations, we used the 3D averaging filter with the pattern matching algorithm. The procedure is the same as explained in Figure S1. As shown in Figures S3c and S3d, the sharp peaks in the original image were removed by the averaging. This smoothing effect is important to suppress excessive enhancement of F_{STA} caused by the $\rho(r)$ to F_{STA} conversion described by the following equation.

$$F_{STA} = \frac{k_B T}{\rho} \frac{\partial \rho}{\partial z}, \tag{3}$$

where k_B and T denote Boltzmann's constant and absolute temperature, respectively. Due to the factor ($\partial \rho / \partial z$) in this equation, sharp peaks in the $\rho(r)$ profiles are excessively enhanced in the $F_{STA}(r)$ profiles. The average filtering is helpful to suppress such excessive enhancement.

The 3D $\rho(r)$ image used in this study has a lateral extent corresponding to 33 unit cells of fluorite(111) surface and pixel spacing of 0.05 nm in xyz directions. After the averaging, we expanded the size of the 3D image by repeating it twice in xyz directions. In addition, we applied a 3 × 3 averaging filter to each xz cross section constituting the 3D image. Figure S3b shows the averaged z cross section. In the image, irregular contrasts in the original image (Figure S3a) are largely suppressed owing to the averaging. In addition, the layer-like contrast corresponding to S4 in the filtered image is much clearer than that in the original image. Figure S3c and S3d show $\rho(r)$

profiles over Ca, F_h and F_l sites obtained from the z cross sections before and after the filtering, respectively. These profiles show that the discontinuities in the original profiles are largely eliminated in the filtered profiles. This should prevent the excessive enhancement caused by the $\rho(r)$ to $F_{STA}(r)$ conversion.
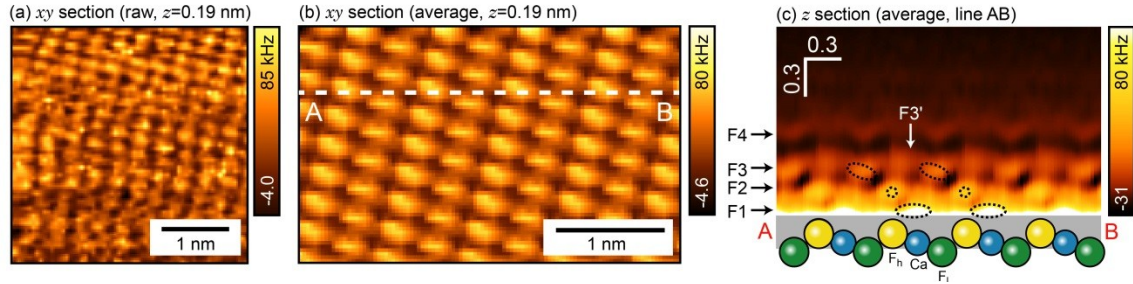
(a) xy section (raw, z=0.19 nm)   85 kHz   -4.0   1 nm

(b) xy section (average, z=0.19 nm)   80 kHz   -4.6   A   B   1 nm

(c) z section (average, line AB)   0.3   0.3   F3'   F4→ F3→ F2→ F1→   80 kHz   -31   A   B F_h Ca F_l

Figure S4: Another example of the 3D Δf images obtained at a fluorite-water interface in pure water. (a, b) xy cross section of the raw and average data. (c) z cross section of the average data.

Figure S4 shows another example of the 3D Δf images obtained at a fluorite-water interface in pure water. In the xy cross section of the raw data, atomic-scale periodic structures are visible. Although the stable imaging condition lasts only for a limited time (< 1 min), we can obtain a 3D average force data from the upper region showing clear atomic-scale contrasts without significant distortion. The xy cross section taken from the average 3D data is shown in Figure S4(b). The z cross section taken along [-1 -1 2] direction (i.e., the line A-B indicated in Figure S4(b)) is shown in Figure S4(c). In the image, we can identify the localized force peaks F1-F3 as well as the layer-like distribution of F4. In addition, we can see an enhanced force distribution corresponding F3' as indicated by an arrow. These features clearly show that the main features discussed in the main text is not the only one data but is reproducible.